Energy 230 (2021) 120845

Contents lists available at ScienceDirect

Energy

journal homepage: www.elsevier.com/locate/energy

In-situ phase separation to improve phase change heat transfer performance

Xiaojing Ma [a, b], Jinliang Xu [a, b], Jian Xie [a, b, *]

[a] Beijing Key Laboratory of Multiphase Flow and Heat Transfer for Low Grade Energy Utilization, North China Electric Power University, Beijing, 102206, China

[b] Key Laboratory of Power Station Energy Transfer Conversion and System, North China Electric Power University, Ministry of Education, Beijing, 102206, China

ARTICLE INFO

Article history:
Received 2 April 2021
Received in revised form
29 April 2021
Accepted 30 April 2021
Available online 6 May 2021

Keywords:
Phase separation
Boiling
Condensation
Critical heat flux
Flow instability

ABSTRACT

Phase change is widely applied in thermal-power conversion, cooling and thermal management, influencing efficiency, safety and cost of energy systems. The complicated mass, momentum and energy exchanges between two-phases causes large pressure drops, critical heat fluxes and flow instabilities. Here, a review on phase separation principle for phase change heat transfer is provided. The phase separation principle is presented in a theoretical form. Design and operation of phase separation for evaporator, condenser and heat pipe are commented. Because phase separation assigns pathways for liquid and vapor, it improves pool boiling performance and eliminates flow instability for micro-evaporator. For micro-condenser, the lined pin fins array creates liquid and vapor passages. The expanded liquid passage adapts increased flow rate to increased flow passage area for liquid. Pin fins are effective for filmwise condensation to increase heat transfer coefficients at low cost of pumping power. Phase separation for macro-condenser was fulfilled by suspending mesh screen membrane tube in condenser tube to confine vapor in annular region, yielding enhanced thin film condensation. Phase separation was commented on smart heat pipe. Superhydrophilic evaporator and superhydrophobic condenser generate nucleate mechanism, achieving increased heat transfer coefficients when heat loads increase. Perspective of phase separation was discussed.

1. Introduction

In nature, matter has three phases of solid, liquid and gas. Physically, the distance between molecules is significantly different for different phases. The transition from one phase to another is called phase change, which is a physical process without chemical reaction. When phase change takes place, energy should be applied to the system or dissipated out of the system. Hence, phase change is an effective way for energy transfer. A Rankine cycle heats water into steam to drive turbine for power generation. Then, the exhaust vapor at turbine outlet is condensed into water, forming a consecutive cycle. To maintain the effective operating of micro-electronics chip, the chip should be well cooled and maintained in an acceptable temperature level. Heat flux that can be dissipated by single phase convective heat transfer is limited. Phase change heat transfer is an effective way to dissipate high heat flux for electronic cooling. For many engineering applications, thermal performance of evaporator and condenser affects the safety, compactness and efficiency of industry facilities [1]. The facilities may be burned out when critical heat transfer is approaching. Heat transfer coefficient determines heat transfer area, which affects the compactness and fabrication cost of heat exchangers. According to the laws of thermodynamics, the vapor temperature and pressure at turbine inlet affect the cycle efficiency. A microchannel evaporator shall cool a microelectronic chip in a reasonable temperature level with acceptable pumping power.

In order to develop efficient nuclear and coal fired power generation technologies, many investigations have been carried out on phase change heat transfer worldwide since 1950–1960s. Nowadays, a semi-theoretical-empirical theory framework has been established for phase change heat transfer due to its complexity. Chen developed a formula to predict boiling heat transfer

* Corresponding author. Key Laboratory of Power Station Energy Transfer Conversion and System, North China Electric Power University, Ministry of Education, Beijing, 102206, China.
E-mail address: xiejian90@ncepu.edu.cn (J. Xie).

https://doi.org/10.1016/j.energy.2021.120845
0360-5442/

Nomenclature

A	area, m_2
$A^*_{AO_1B}$	area of sector AO_1B in Fig. 1, m^2
$A^*_{DO_1E}$	area of sector DO_2E in Fig. 1, m^2
C	empirical coefficient, see Eq. (4)
C_1 and C_2	arc lengths in Fig. 1, m
C_p	specific heat at constant pressure, J/(kg K)
CHF	critical heat flux, W/m^2
d	sphere diameter of particle, m
d_p	diameter of mesh pore, m
D	tube diameter, m
EF	heat transfer enhancement ratio
f	oscillation frequency, Hz
F_m	evaporation momentum force, N
g	gravitational acceleration, m/s^2
G	mass flux, $kg/(m^2s)$
G_{Gibbs}	Gibbs free energy, J
h	heat transfer coefficient, $W/(m^2K)$
h_{lv}	latent heat of evaporation, J/kg
H	height of pin fin, m
H_l	liquid height in tube bottom in Fig. 5c, m
k	thermal conductivity of liquid, W/(mK)
l_1 and l_2	the lengths of vapor covering pin fin, m
l_{unit}	length of unit, m
L	side length of pin fin, m
m	mass, kg
m_c	cooling water flow rate (kg/s)
P	pressure, Pa
ΔP_{12}	capillary pressure, Pa
ΔP_f	frictional pressure drop, Pa
PEC	performance evaluation coefficient
q	heat flux, W/m^2
Q	heat load, W
r	radial direction, m
S_g	area exposed in vapor, m^2
S_n	non-dimensional oscillation amplitude
t	time, s
T	temperature, K
ΔT	wall superheat, K
V	bubble volume, m^3
w	bubble width in Fig. 3c, m
W	width of bare channel in Fig. 3c, m
W_{porous}	width of porous pin fin region, m
x	vapor mass quality or flow direction, m
X	Martinelli number
y	perpendicular direction of flow, m
z	height direction of channel, m

Greek symbols

α	void fraction or an exterior angle of triangle BO_1F in Fig. 1
β	The angle between y direction and the inclined side wall of pin fin
δ	liquid film thicknesses, m
φ^2_{lo}	two-phase multiplier coefficient
γ	surface tension, N/m
λ	distance between neighboring pin fins, m
θ	contact angle or conical angle in Fig. 4a
ρ	density, kg/m^3

Subscript

1, 2	state 1 or 2 in Fig. 5b
A, B	cross section A-A or B-B in Fig. 5c
ave	average
BO_1F	triangle BO_1F in Fig. 1
c	condenser
CDEF	rectangular CDEF in Fig. 1
DO_2E	triangle DO_2E in Fig. 1
e	evaporator
f	friction pressure drop
g	gas
in	inlet
l	liquid
lv	liquid-vapor interface
net	net force
osc	oscillation
s	solid
sv	solid-vapor interface
sl	solid-liquid interface
TP	two-phase flow
v	vapor
w	wall
x	x direction
y	y direction

coefficient, adjoining nucleate boiling mechanism and convective heat transfer mechanism. The formula is widely applied to support the development of steam power technologies [2]. With fast development of global microelectronics industry since 1980–1990s, phase change in microchannels has become a hot research topic. It is expected that the heat flux of microelectronics will reach 1–10 kW/cm^2 in the future, which is a challenge for heat transfer [3]. To solve the energy and environmental issues since 21st century, the research and development are enhanced worldwide to develop efficient energy systems. Steam power engineering is one of the most popular technologies for power generation, in which evaporator and condenser are two key components to operate a power cycle, for which phase change heat transfer faces new challenges. In concentrated solar power station, solar receiver works at high radiation heat flux. The heat transfer enhancement, flow rate distribution and flow instability in parallel tubes of solar receiver should be paid great attention [4]. Low grade energy utilization presents strict requirement for phase change heat transfer. For such applications, due to small temperature difference between hot side fluid and cold side fluid of heat exchangers, the heat transfer area should be large, increasing the cost of heat exchangers to prevent the commercial applications of energy saving products. Hence, novel idea should be proposed to decrease the cost for low grade energy utilization. Organic fluids with low boiling point are widely used in heat pumps, air conditioners and organic Rankine cycle. Heat transfer coefficients of phase change are lower than those of convective heat transfer of water. It is strongly desired to increase phase change heat transfer coefficient and decrease pressure drop for organic fluids [5].

To decrease energy consumption by buildings, solar absorbers receive solar energy on the roof of buildings, and transfer heat into buildings, yielding heat loss during heat transfer process. Available heat pipes may not work due to the difficulties in transferring heat from high position to low position. An anti-gravity heat pipe with its length in the range of 1–10 m would be perfect to act as the heat transfer device [6]. In the aerospace field, the operating condition

for key components of aircraft is becoming more serious, and the heat flux of the leading edge of scramjet engine is as high as 100 kW/cm^2, thus there is an urgent need for the development of thermal protection technology [7]. Under microgravity environment, liquid film thickness is larger than that under earth gravity condition, increasing the weight and volume of condensers to raise the launch and operation costs [8]. Heat pipe works well under earth gravity condition. Under microgravity condition, the performance of heat pipe is deteriorated, under which surface tension force is only the driving force for fluid circulation due to negligible gravity force.

The above literature survey shows the following trends on research and development of phase change heat transfer: (1) High heat flux that can be dissipated by phase change heat transfer is required. (2) Heat transfer coefficient should be as high as possible, which should be accompanied by a low cost of the rise of pressure drops. Pressure drops should be as low as possible. (3) Flow instability related to phase change heat transfer should be eliminated.

Phase change heat transfer is more complicated than single-phase convective heat transfer. To enhance phase change heat transfer, the traditional methods are to fabricate micro structures such as internal threads and grooves on internal walls of tubes, which have been successfully applied in industries [9]. Dropwise condensation on superhydrophobic surface has been widely investigated worldwide. However, micro/nano structures of superhydrobic surface may be spoiled after long-term operation. Thus, dropwise condensation has not been commercialized. The practical condensers still work with filmwise condensation [10]. Heat pipe may contain porous media structure such as grooves, sintering wires or powders [11]. Pores with single length scale cannot overcome the conflict between smaller length scale for liquid supplement and larger length scale for vapor venting. It is necessary to break through the traditional theory and technical framework, searching new solutions to improve phase change heat transfer.

During phase change, a specific volume is occupied either by vapor or by liquid. The spatial-time phase distribution is a key scientific issue. In a local region, volume void fraction is defined as the gas volume divided by the total volume. Alternatively, surface void fraction is defined as the cross-sectional area occupied by gas divided by the total cross-sectional area. To improve the phase change heat transfer performance, one needs to modulate the spatial-time phase distribution. The target is to overcome the conflict induced by single length scale that cannot adapt to various processes or phenomena. For this consideration, phase separation for phase change heat transfer has been proposed and investigated in the authors' group in the past ten years. Initially, phase separation for in-tube condensation heat transfer was proposed and investigated. Mesh membrane tube is suspended in condenser tube, dividing the tube cross section into an annular region near the wall and a core region inside the membrane tube. The phase separation condenser was awarded by an US patent [12]. The miniature mesh pores prevent gas bubble from entering the mesh membrane tube but capture liquid into the mesh membrane tube, ensuring largest possibility for tube wall contacting with gas to form perfect thin liquid film condensation. Adiabatic gas-liquid two-phase flow experiment and heat transfer experiment were systematically performed [13–15], showing that heat transfer coefficients can be increased to 1.82 times of those in bare tubes without membrane tube insert [16].

Subsequently, phase separation for microchannels based evaporator and condenser was invented and investigated. Porous-wall-microchannels evaporator was proposed to include pin-fin region and bare channel region [17]. The former acts as bubble nucleation and growth, and the latter functions as vapor collection and transportation. When bubbles are crossing the interface between pin fin region and bare channel, they move to bare channel driven by surface energy. Because pressures can be transmitted from pin fin region to bare channel due to the pressure difference across the two regions, bubbles in bare channel are squeezed to generate space for liquid transportation. Hence, bubble blockage, which is serious in conventional microchannels, is completely eliminated to suppress flow instability in evaporators [17].

Micro-condenser using phase separation concept was investigated [18]. Lined pin fin arrays generate liquid passages and vapor passages alternatively in chip width direction. The decreased Gibbs free energy with gas–liquid interface advancing pin fin throat location is the mechanism to induce liquid flow from vapor passages to liquid passages. Parallel phase separation condenser (PPS with constant cross sections of fluid passages) and conical phase separation condenser (CPS with varied cross sections of fluid passages) were demonstrated. During the vapor condensing process, mass flow rates of liquid and vapor increase and decrease, respectively. For PPS, pin fins array may be exposed by liquid to make the pin fins not effective for heat transfer. CPS effectively adapts the varied flow rates of the two-phases to the varied cross sectional areas of the two-phases. Hence, half-side of pin fins is exposed by vapor which is effective for condensing [18].

Phase separation was introduced to heat pipe, yielding smart heat pipe having capability to increase heat transfer coefficients response to the increase of heat loads [19]. The phase separation is fulfilled by wettability match between superhydrophilic evaporator and superhydrophobic condenser. Because evaporator wick is full of liquid, nucleate boiling mechanism occurs in evaporator, increasing heat transfer coefficients when heat flux increases. Meanwhile, condenser surface is exposed by vapor, nucleate condensation mechanism takes place, raising heat transfer coefficients when heat load increases. In such way, heat transfer coefficients of both evaporator and condenser are increased for increment of heat loads [19]. In this paper, the principle and application of phase separation are systematically reviewed, including not only our own works, but also works performed by other research groups worldwide.

2. Current options and barriers

Phase change involves several issues such as courante of critical heat flux (*CHF*), flow instability, large pressure drop and thick liquid film thickness, which severely deteriorate the facilities performance. This section presents a short review on these issues. Hence, one can understand why phase separation should be introduced into phase change heat transfer.

Critical heat flux (*CHF*): As an important parameter characterizing the evaporator performance, critical heat flux (*CHF*) specifies the up-limit of heat flux that can be sustained by evaporator. When heat flux approaches *CHF*, the heater surface is covered by a vapor layer, yielding the Leidenfrost phenomenon. The heater surface may be burned out due to small thermal conductivity of vapor. Hence, *CHF* should be avoided for practical operations. The *CHF* mechanism is very complicated. Zuber [20] developed a theoretical formula to predict *CHF* on smooth surface. He assumed that when *CHF* is approaching, the distance between neighboring vapor columns approaches the wavelength of the Rayleigh-Taylor instability, under which liquid cannot rewet the heater surface. The expression is as follows:

$$CHF = \frac{\pi}{24}\sqrt{\rho_v} h_{lv} \sqrt[4]{\gamma_{lv} g(\rho_l - \rho_v)} \quad (1)$$

where h_{lv}, ρ_l, ρ_v, γ_{lv}, g are the latent heat of evaporation, liquid density, vapor density, surface tension of liquid-vapor interface and gravitational acceleration, respectively. Based on this model, *CHF* for water boiling on smooth surface at atmospheric pressure is ~110 W/cm^2. Many works have been done to modify the Zuber's model, thus *CHF* can be predicted on enhanced structure surface [21]. For boiling heat transfer, counter-current flow occurs during vapor venting and liquid supplement. The vapor venting makes it difficult for liquid supplement towards heater surface, which is a fundamental mechanism to trigger *CHF* [22]. Compared to pool boiling, convective boiling is more complicated. For annular flow in convective boiling tubes, the whole cross-section of the tube is occupied by vapor with droplet entrainment. Liquid film on the tube wall may be dried out at high vapor mass quality. If dry spots on tube walls cannot be rewetted by liquid, *CHF* is triggered [23]. Liquid droplets entrained in vapor and impacting on tube walls influence the occurrence of *CHF*. No matter for pool boiling or convective boiling, *CHF* is strongly related to that whether tube walls can be rewetted by fresh liquid. Thus, the modulation of spatial-time phase distribution to keep wetting of tube walls is a key consideration to delay *CHF*.

Boiling instability: Boiling instability involves oscillation of several parameters such as flow rate, temperature and pressure. Flow instability may cause thermal stress to damage facilities. Hence, it should be avoided for practical operation. From the 1950s to 1980s, many works have been done on boiling heat transfer in large diameter tubes. Several instabilities such as pressure drop oscillation, density wave oscillation and thermal oscillation were identified [24]. After 2000, many authors investigated boiling instability in microchannels, including Professor Ping Cheng's work and the authors' work [25,26]. In order to understand similarities and differences of boiling instabilities in large diameter tubes and microchannels, boiling in microchannels was investigated by synchronous measurement of wall temperatures with infrared radiation (IR) camera and flow patterns with high speed camera, incorporating the wavelet decomposition technique [27]. The collected signals were decoupled in three time scales. The pressure drop oscillation and density wave oscillation are identified, which are similar to those occurring in larger diameter tubes. However, transient liquid film oscillation is unique for boiling in microchannles. The pressure drop oscillation is related to compressible volume in the upstream of test section. When the characteristic length of channels such as tube diameter is smaller than capillary length, which is ~2.7 mm for water at atmospheric pressure, the channel cross-section is occupied by bubble to cause bubble blockage, amplifying the pressure drop oscillation. The traditional method to suppress pressure drop oscillation is to arrange orifice restriction at channel inlet, at the cost of the increment of pressure drop across test section [28]. The phase separation principle is a break-through method to suppress flow instabilities, which will be described latter.

Pressure drop of two-phase flow: In phase change system, there exist complicated interactions of mass, momentum and energy across gas-liquid interface. As a non-dimensional parameter, the Martinelli number characterizes the ratio of friction pressure drop of gas phase with respect to that of liquid phase:

$$X^2 = \left(\left|\frac{dP}{dx}\right|_f\right)_l \Big/ \left(\left|\frac{dP}{dx}\right|_f\right)_g \quad (2)$$

The frictional pressure drop of two-phase flow is

$$\Delta P_{f,TP} = \Delta P_{f,l}\varphi_{lo}^2 \quad (3)$$

where $\Delta P_{f,1}$ is the friction pressure drop assuming the whole two-phase mixture flowing as liquid only, φ_{lo}^2 is the two-phase multiplier coefficient:

$$\varphi_{lo}^2 = 1 + \frac{C}{X} + \frac{1}{X^2} \quad (4)$$

where C is a coefficient determined by experiment.

Many investigations show that φ_{lo}^2 ranges from 10 to 100, indicating friction pressure drop of two-phase fluid one to two magnitudes larger than that of single-phase liquid flow. As reported by Parmar & Majumder [29] and the author's work [18], the frictional pressure drop of two-phase flow is related to interfacial area between liquid and gas. Larger interfacial area increases the energy dissipation to raise shear force between the two-phases. It is concluded that phase separation significantly reduces interfacial area between two-phases for the reduction of pressure drops, which is verified by our experiments [18].

Liquid film condensation: Condensation heat transfer is widely applied in power generation systems, air conditioners and heat pipes. Most metallic materials such as stainless steel and copper are hydrophilic to liquid such as water. For convective condensation, filmwise condensation is a dominant mechanism. Grooved tubes, threaded tubes, micro-needle ribs tubes [9,30,31], twisted elliptical tubes, special-shaped pipes [32] and others [33,34] are widely applied to enhance single-phase convective heat transfer, which are also extended for condensation heat transfer, but they do not take account of unique characteristic of two-phase flow. In 1916, Nusselt noted that the condensation heat transfer coefficient h is inversely proportional to liquid film thicknesses δ [35]:

$$h = \frac{k}{\delta} \quad (5)$$

where k is the thermal conductivity of liquid.

Convective condensation heat transfer in tubes is influenced by the flow pattern "vapor in the core and liquid on the wall", which dominates liquid film thickness. It is expected that the modulation of phase distribution with "liquid in the core and vapor near the wall", forms thin liquid film thickness to maximize condensation heat transfer coefficient [12].

3. Fundamental consideration of phase separation

Heat transfer enhancement involves active method and passive method [36]. The former needs external electric field [37], magnetic field [38] or ultra-sonic activation [39], but the latter does not need external excitation. For large scale utilization such as thermal-power conversion, passive method is preferable. The present paper mainly deals with phase separation using structure gradient, belonging to passive method. Latter it will be shown that there are several methods to fulfill phase separation, including gravity driven effect [40–42], evaporation momentum force [43,44] and surface energy driven flow [12,45]. Among them, the surface energy driven flow is a preferable method because it is reliable and can be extended for various applications. As an example, an analysis for phase separation is presented when a bubble is crossing a junction between pin fins region and bare channel region, which has been applied to micro-evaporator (see Fig. 1) [45]. Each pin fin has a rectangular cross section with a length of L. The fin height is H. The distance between neighboring pin fins is λ. The characteristic contact angle is θ between pin fin and the working liquid. The angle

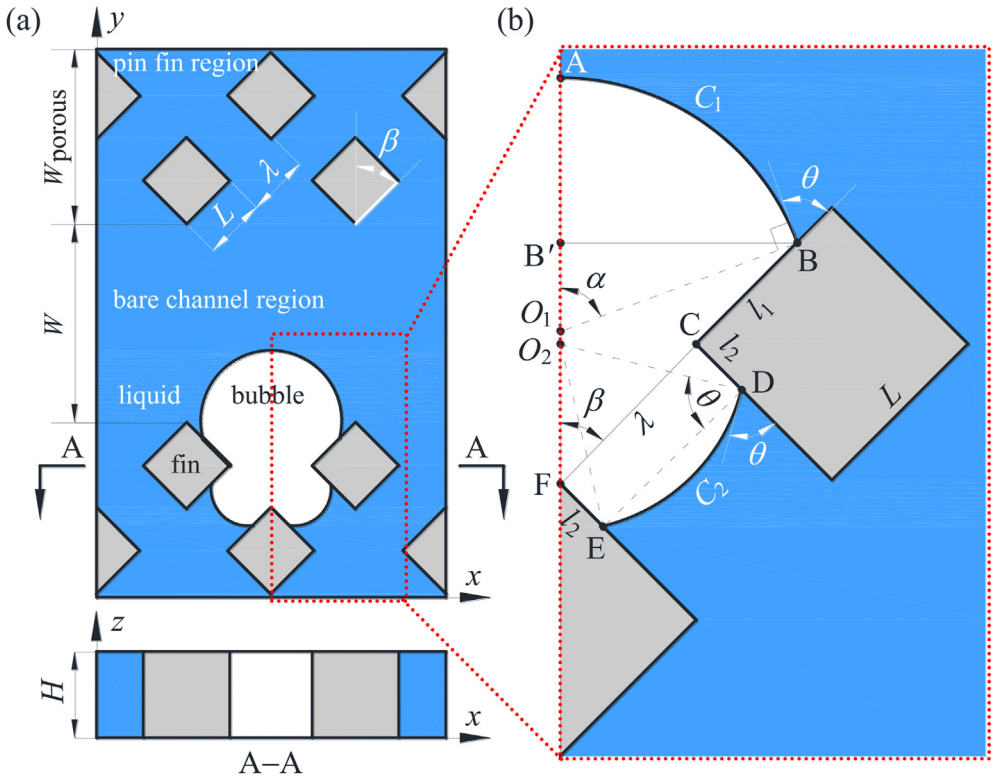

Fig. 1. Phase separation principle demonstrating a bubble penetrating out of the pin fins region to bare channel region.

between the symmetry line perpendicular to flow direction x and the inclined side wall of pin fin is β. A bubble is penetrating from pin fin gap to bare channel. For the pin fin closest to bare channel, the vapor covering lengths are l_1 and l_2, respectively. O_1 and O_2 are the center points of the vapor-liquid interface curvature $\overset{\frown}{AB}$ and $\overset{\frown}{DE}$, respectively. C_1 and C_2 are the arc lengths of $\overset{\frown}{AB}$ and $\overset{\frown}{DE}$.

Our analysis includes the determination of Gibbs free energy of system (G_{Gibbs}) and verification of the criterion $\frac{\partial G_{\text{Gibbs}}}{\partial l_1} < 0$. If the criterion is satisfied, the bubble interface automatically moves towards bare channel due to the decrease of G_{Gibbs} when l_1 increases. Besides, factors influencing the sign (positive or negative) of G_{Gibbs} are to be analyzed. The G_{Gibbs} is

$$G_{\text{Gibbs}} = A_{\text{lv}}\gamma_{\text{lv}} + A_{\text{sv}}\gamma_{\text{sv}} + A_{\text{sl}}\gamma_{\text{sl}} \tag{6}$$

where γ is the surface tensions and A is the contact area. The subscripts s, l and v represent solid, liquid and vapor, respectively. The Young equation writes

$$\cos\theta = \frac{\gamma_{\text{sv}} - \gamma_{\text{sl}}}{\gamma_{\text{lv}}} \tag{7}$$

Substituting Eq. (7) into Eq. (6) yields

$$G_{\text{Gibbs}} = (A_{\text{sl}} + A_{\text{sv}})\gamma_{\text{sl}} + (A_{\text{sv}}\cos\theta + A_{\text{lv}})\gamma_{\text{lv}} \tag{8}$$

The three contact areas are

$$A_{\text{lv}} = 2H(C_1 + C_2),\ A_{\text{sv}} = 2H(l_1 + 2l_2), A_{\text{sl}} = 2H[L - l_1 + 2(L - l_2)] \tag{9}$$

The geometric parameters have the following relationships

$$C_1 = \frac{(\lambda + l_1)\sin\beta}{\sin\alpha}\alpha \tag{10}$$

$$\alpha = \beta + \frac{\pi}{2} - \theta \tag{11}$$

$$C_2 = \frac{\lambda}{2\cos\theta}(\pi - 2\theta) \tag{12}$$

Substituting Eq. (9)–(12) into Eq. (8) yields

$$G_{\text{Gibbs}} = 6HL\gamma_{\text{sl}} + 2H\gamma_{\text{lv}}\left[(l_1 + 2l_2)\cos\theta + \frac{(\lambda + l_1)\sin\beta}{\sin\alpha}\alpha + \frac{\lambda(\pi - 2\theta)}{2\cos\theta}\right] \tag{13}$$

The partial differential of Eq. (13) with respect to l_1 is

$$\frac{\partial G_{\text{Gibbs}}}{\partial l_1} = 2H\gamma_{\text{lv}}\left[\cos\theta + \frac{\sin\beta}{\sin\alpha}\alpha\right] + 4H\gamma_{\text{lv}}\cos\theta\frac{\partial l_2}{\partial l_1} \tag{14}$$

In Eq. (14), all the parameters are known except $\frac{\partial l_2}{\partial l_1}$. Using the conservation of bubble volume at different time, one achieves the relationship between l_1 and l_2. The bubble volume V is

$$V = 2H\left(A^*_{AO_1B} + A_{BO_1F} + A_{CDEF} + A^*_{DO_2E} - A_{DO_2E}\right) \tag{15}$$

where $A^*_{AO_1B}$,A_{BO_1F}, A_{CDEF}, $A^*_{DO_2E}$ and A_{DO_2E} are the areas of sector AO_1B, triangle BO_1F, rectangular CDEF, sector DO_2E and triangle DO_2E, which are as follows

$$A^*_{AO_1B}=\frac{(\lambda+l_1)^2\alpha}{2}\left(\frac{\sin\beta}{\sin\alpha}\right)^2, A_{BO_1F}=\frac{(\lambda+l_1)^2}{2}\left(\sin\beta\cos\beta-\sin^2\beta\frac{\cos\alpha}{\sin\alpha}\right),$$
$$A_{CDEF}=\lambda l_2, A^*_{DO_2E}=\frac{1}{8}\left(\frac{\lambda}{\cos\theta}\right)^2(\pi-2\theta), A_{DO_2E}=\frac{\lambda^2}{4}\tan\theta \tag{16}$$

Substituting Eq. (16) into Eq. (15) yields

$$l_2=\frac{V}{2H\lambda}-\frac{(\lambda+l_1)^2}{2\lambda}\left[\left(\frac{\sin\beta}{\sin\alpha}\right)^2(\alpha-\sin\alpha\cos\alpha)+\sin\beta\cos\beta\right]-\frac{\lambda}{8\cos\theta}\frac{\pi-2\theta-2\sin\theta\cos\theta}{\cos\theta} \tag{17}$$

$$\frac{\partial l_2}{\partial l_1}=-\frac{\lambda+l_1}{\lambda}\left[\left(\frac{\sin\beta}{\sin\alpha}\right)^2(\alpha-\sin\alpha\cos\alpha)+\sin\beta\cos\beta\right] \tag{18}$$

Substituting Eq. (18) into Eq. (14) yields

$$\frac{\partial G_{Gibbs}}{\partial l_1}=2H\gamma_{lv}\left\{\cos\theta-2\cos\theta\frac{\lambda+l_1}{\lambda}\left[\left(\frac{\sin\beta}{\sin\alpha}\right)^2(\alpha-\sin\alpha\cos\alpha)+\sin\beta\cos\beta\right]+\frac{\sin\beta}{\sin\alpha}\alpha\right\} \tag{19}$$

Eq. (19) judges if the criterion of $\frac{\partial G_{Gibbs}}{\partial l_1}<0$ can be satisfied, involving the geometry parameter of pin fin λ, the fin arrangement parameter β and the contact angle θ, noting that α is determined by Eq. (11). Citing the parameters from Ref. [45] with $H=75$ μm, $\lambda=15$ μm, $\beta=45^o$ and $\theta=40^o$, $\frac{\partial G_{Gibbs}}{\partial l_1}=-1.84\times10^{-6}$ J/m <0, explaining the effective phase separation for micro-evaporator applications.

4. Phase separation for various applications

Here, the method and effectiveness of phase separation are described for pool boiling, micro-evaporator, micro-condenser, convective condenser tube and heat pipe.

4.1. Phase separation for pool boiling

Pool boiling attracts many interests in heat transfer society. The investigation of pool boiling forms the foundation to deepen the understanding of convective boiling in channels. At high heat fluxes, the key to improve the performance of pool boiling lies in supplying liquid towards heater surface to prevent the occurrence of dry spots. Conventional methods to enhance pool boiling heat transfer are to construct various structures such as micro-grooves, pin fins and porous media on heater surface. Pores of these structures have single length scale, which cannot satisfy the requirement that different processes or phenomena should adapt to different scales for pore sizes. Liquid is sucked into porous media with the help of surface tension force. The smaller the pore size, the larger capability for liquid suction is. However, smaller pores not only create addition viscous resistance for liquid suction, but also increase the resistance for vapor venting out of the porous media. Hence, the structured surface with single length scale pores has the limited capability to raise *CHF*. Usually, *CHF* on enhanced structured surface are smaller than two times of those on plain surface [22].

In order to overcome the conflict between liquid supply and vapor venting, the present authors proposed the 3D mastoid process array surface to enhance pool boiling heat transfer, inspired by the structure on petal of Dahlia Pinnata flower from nature (see Fig. 2a–c) [46]. The mastoid processes are sintered on heater substrate using uniform or non-uniform metallic powders. It is shown that multiscale pores can be formed inside mastoid processes, even using uniform particles sintering. Considering that three spheres with identical size are stacked with each other in space, the central circle which is tangent to all the three spheres has a diameter of 0.15d, where d is the sphere diameter. Thus, the 15 μm pores can be formed when using particle size of 100 μm, which is helpful for liquid suction. The sintering process of ~100 μm particles also creates larger cracks with pore size of ~100 μm, which are beneficial for vapor venting from mastoid process into liquid pool. The multiscale sintering structure significantly increases pool boiling heat transfer coefficient. Meanwhile, *CHF* on such surface can be 3.7 times of those on plain surface. The above improvement is deduced from the reasonable assignment of flow paths for vapor phase and liquid phase. It is interest to observe hollow wells, which are actually the concave vapor-liquid interface during vapor venting from the tips of mastoid process. The hollow well structures are useful for liquid supplement under high heat flux operation. It is noted that the particles sintering is a mature technique, which can be widely applied for heat pipe applications.

Three mechanisms of transient conduction, microconvection and microlayer evaporation are involved in pool boiling. Which mechanism dominates heat transfer is still a debate. To enhance microconvection, Kandlikar proposed heterogeneous pin fins structure, consisting of vertical fin surrounded by inclined and curved island structure (Fig. 2d–f) [43]. The heat transfer improvement is related to evaporation momentum force resulting from the density difference of liquid and vapor at an evaporating interface. The resulting fast interface motion creates evaporation momentum force, directing bubbles to move along the inclined island solid structure, not moving upwards. In such a way, the flow paths of liquid and vapor are separated for efficient vapor escaping and liquid supplement. The heat transfer coefficient achieved 629

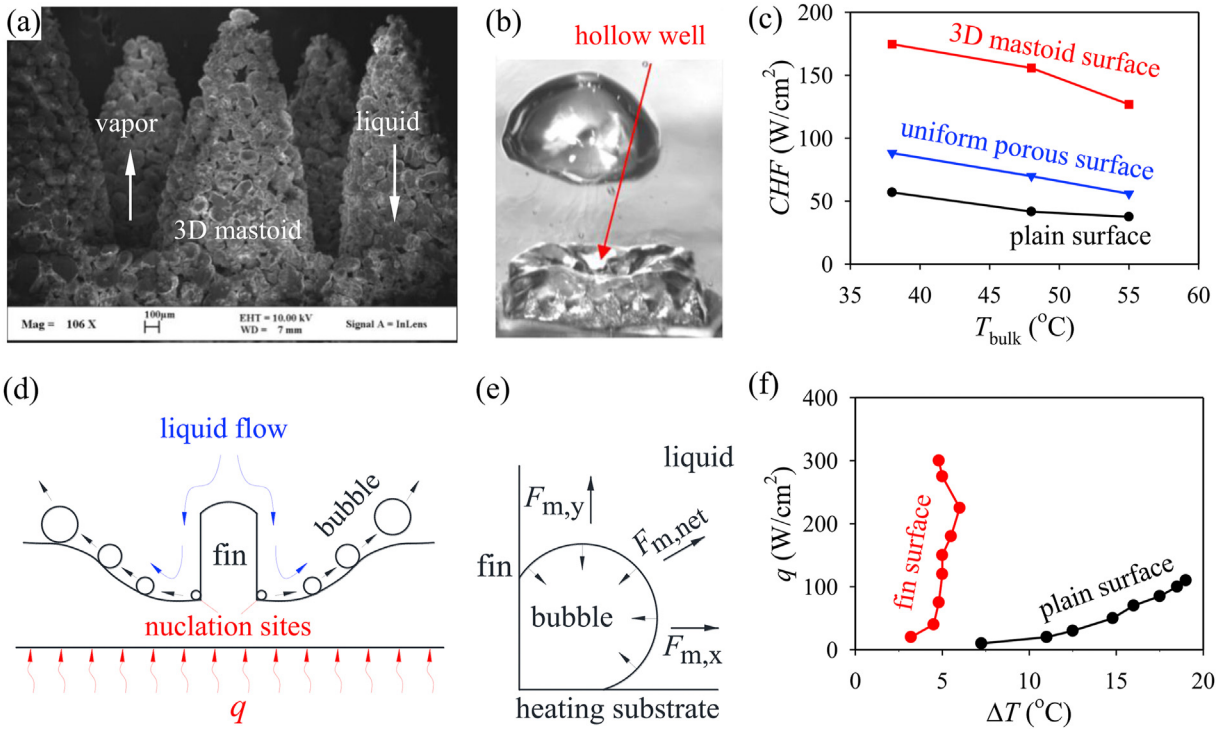

Fig. 2. Phase separation for pool boiling heat transfer (a: 3D mastoid processes array [46]; b: hollow well just after bubble departure [46]; c: *CHF* on various surfaces [46]; d: heterogeneous fins for phase separation [43]; e: evaporation momentum force by heterogeneous fins [43]; f: boiling curves on heterogeneous fins surface and plain surface [43]). Subfigures a–c are reprinted with permission from Ref. [46], Elsevier. Subfigures d–f are reprinted with permission from Ref. [43], AIP Publishing.

kW/m^{2}K, which is 12.5 times of that on bare surface. The *CHF* is 300 W/cm^2, which is 2.5 times of that on bare surface [43]. Jaikumar & Kandlikar improved *CHF* to 420 W/cm^2 and heat transfer coefficient to 2900 kW/m^{2}K for water boiling at atmospheric pressure by utilizing phase separation technique [44].

For pool boiling, phase separation is an effective strategy to avoid counter-current flow. There are several methods to fulfil phase separation. Dai et al. [47] sintered mesh screen based micro-membrane on top fin surface of microchannels. Membrane pores enhance liquid suction due to capillary action but prevent vapor venting in vertical direction. Vapor is collected in microchannel grooves and discharged into pool liquid along the side direction of microchannels. Compared with mono-porous evaporating surfaces such as microchannels and copper woven mesh laminates in the same thickness under similar working conditions, *CHF* was substantially increased by 83% and 198%, respectively. Recently, there are also researchers conducting pool boiling studies on structured surfaces with hybrid thermal conductivity or hybrid wettability patterns to realize the phase separation. Rahman et al. [48] fabricated a bi-conductive surface, comprising rows of low-conductivity epoxy embedded into high-conductivity copper substrates. Thus, a spatial ordering of the flow field is formed on the heater, resulting in a fivefold improvement of boiling heat transfer coefficient and two times higher critical heat flux than that of a bare copper surface, respectively. Inspired by the opuntia microdasys and desert beetle which can survive in highly arid environments, Ma et al. [49] proposed a bio-inspired hybrid wettability patterned micro-pillar surface. They studied pool boiling heat transfer on four kinds of heat sinks with different wettability patterns by the latest version of the liquid-vapor phase-change lattice Boltzmann model. It is found that the bio-inspired heat sink with hydrophobic pillar tops and hydrophilic base has the best boiling heat transfer performance which is due to the orderly separation of vapor and liquid paths.

Most of applications use solid wall microchannels as extended heat transfer surface to enhance heat transfer, limiting capillary wicking for liquid supply towards high heat flux substrate. To overcome this limitation, Xu et al. [50] proposed double layers porous wick for loop heat pipe applications. Instead of solid wall microchannels, porous wall microchannels are acted as the bottom layey, which is sintered together with a top sintering membrane layer. The double-layers porous structure not only fulfills phase separation, but also singnificantly enhances the capillary wicking directly towards the heating substrate. Compared with uniform and single layer porous cover on substrate, the double layer porous coating surface with bottom grooves achieved a temperature decrease of 20–50 °C at moderate or high heat loads. The loop heat pipe with this structure attained an evaporator temperatureeee of 63 °C at a heat load of 200 W under anti-gravity operation, which is attractive for micro-gravity applications [51]. Liter and Kaviany's theoretical work indicates that the 3D modulated mastoid processes array could increase the critical heat flux by five times compared to solid wall microchannels, and twenty times compared to bare surface [22]. Hence, it is conclude that phase separation not only increases boiling heat transfer coefficients, but also raises critical heat fluxes, compared to conventional methods.

4.2. Phase separation for micro-evaporator

Boiling instability causes serious fluctuations of pressures, flow rates and temperatures, which should be avoided for practical operation. In this section, the phase separation principle and pressure switch between neighboring channels are described to suppress flow instabilities for micro-evaporator. When the hydraulic diameter of channels is smaller than the capillary length of liquid, the whole cross section of channels is occupied by bubble with a thin liquid film on channel walls. When considering

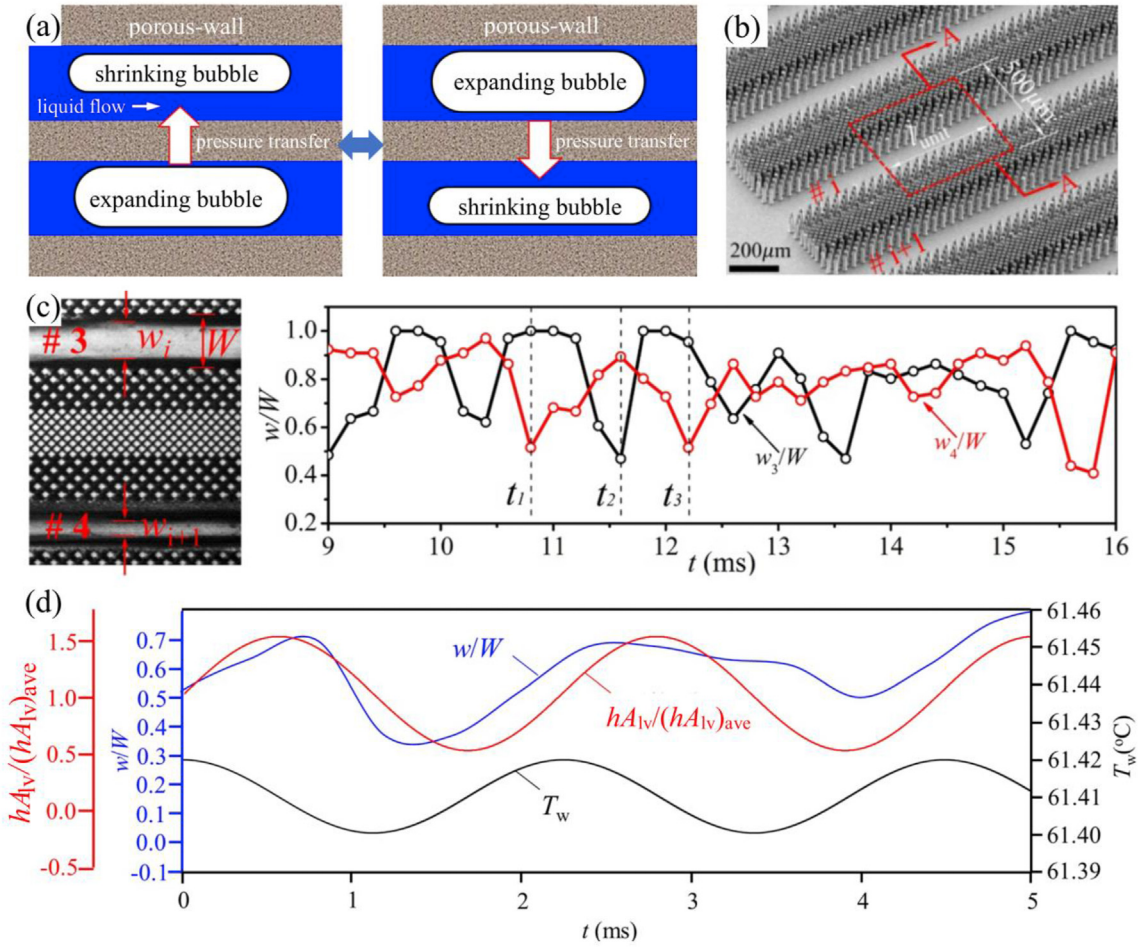

Fig. 3. Phase separation for micro-evaporator [17] (a: pressure switch effect among neighboring bare channels; b: SEM image of porous-wall microchannel evaporator; c: bubble confinement ratio w/W in neighboring channels, where w is the bubble width and W is the channel width; d: convective heat transfer intensities, bubble confinement ratio and wall temperatures versus time). Reprinted with permission from Ref. [17], Elsevier.

multichannels, vapor blockage in one channel decreases flow rate in this channel, but increases flow rates in other channels assuming constant flow rate as a total, generating non-uniform distribution of flow rates in different channels. An academic term called symmetry breaking refers to non-symmetry phenomenon when considering exact symmetry boundary condition [52]. The symmetry breaking influences mass, momentum and energy exchanges among different channels to trigger flow instabilities. For conventional multichannels, the above exchanges take place at the inlet and outlet of channels only.

To eliminate boiling instability, the micro-evaporator working with phase separation principle and pressure switch effect was proposed and investigated [17]. Solid wall microchannels are replaced by porous wall microchanels. Thus, the micro-evaporator includes porous wall regions and bare channel regions. When a bubble is crossing the interface between porous wall region and bare channel region, the surface energy drives the bubble moving into bare channels. Hence, porous wall regions are occupied by liquid, while vapor is occupied in bare channels to fulfil phase separation (see Fig. 3a). Resistance exists for liquid flowing in porous wall regions, leaving a portion of liquid flowing in bare channels. In a specific channel, bubble expansion causes higher pressure than neighboring channels. Due to the connected multi-channels via porous wall, a higher pressure in a bare channel can be transmitted into neighboring bare channels in width direction, squeezing bubble in neighboring bare channel to form a liquid flow passage as a portion of the whole cross section of the bare channel. Thus, bubble expansion in one bare channel should correspond to bubble contraction in neighboring bare channel to suppress bubble blockage. Bubbles become fat and slim in bare channels to generate high frequency "eye-blinking oscillation", yielding ultra-stable heat transfer in micro-evaporator. Because the "eye-blinking oscillation" is related to pressure switch among different channels, this phenomenon is also called the pressure switch effect.

The micro-evaporator was fabricated by MEMS (micro-electricalmechanicalsystem) technique. Boiling experiments were performed with acetone as the working fluid (see Fig. 3b). The bubble confinement ratio is defined as w/W, where w and W are the bubble width and bare channel width, respectively. For solid wall microchannels, the bubble confinement ratio approaches 1. When porous walls are introduced, the bubble confinement ratio is obviously smaller than 1. Phase angles of bubble confinement ratios in neighboring bare channels are experimentally identified to be π, indicating bubble expansion and contraction in alternative channels and pressure switch effect (see Fig. 3c). It is confirmed that the "eye-blinking" oscillation belongs to density wave oscillation propagating in the channel width direction. Because porous-wall width is much smaller than channel length, the "eye-blinking" frequencies are 10–100 times higher than that of the axially propagated density wave oscillation. The "integration parameter

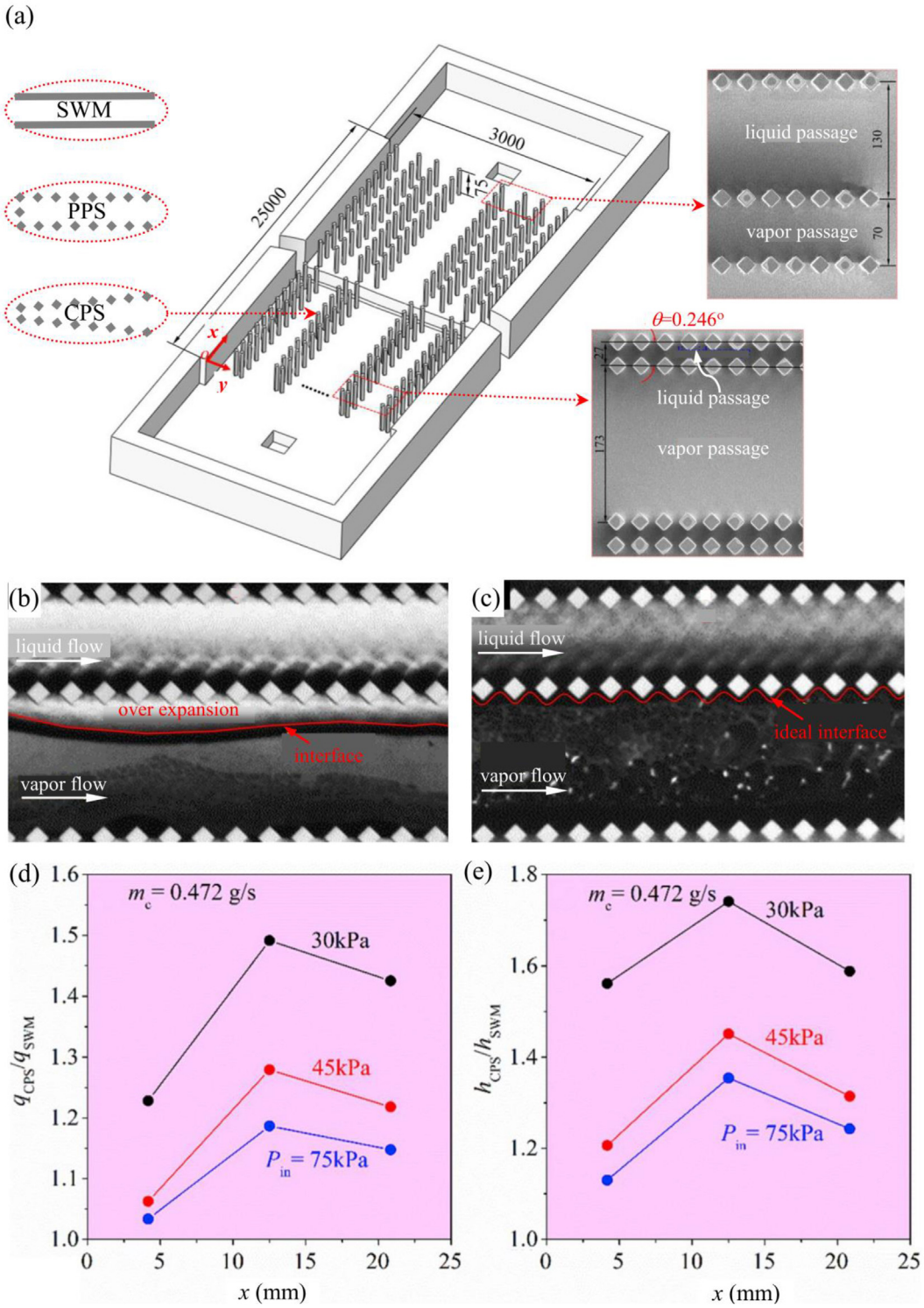

Fig. 4. Phase separation for micro-condenser [18] (a: CPS, PPS and SWM structures; b: liquid over expansion in vapor passage with PPS; c: vapor-liquid interface pinned along the lined pin fins array with CPS; d–e: heat transfer enhancement of CPS compared with SWM). Reprinted with permission from Ref. [18], Elsevier.

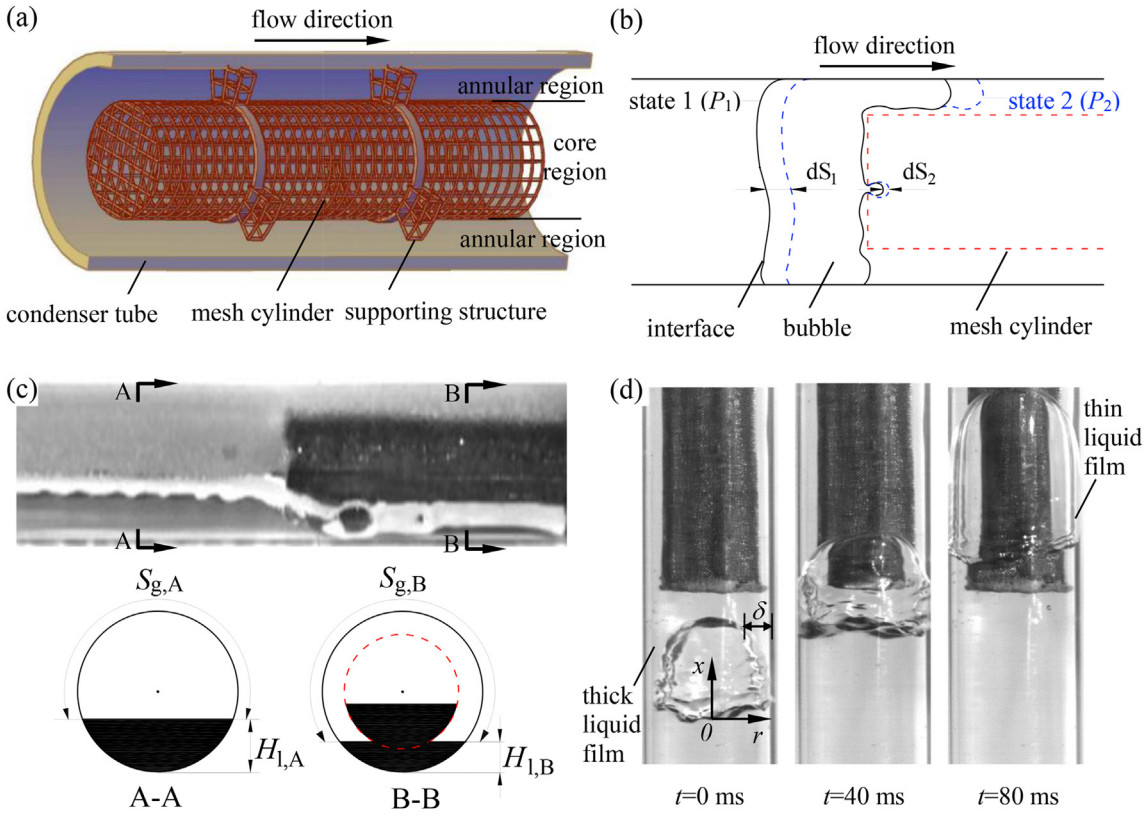

Fig. 5. Phase separation condenser (a: design of phase separation condenser [13]; b: capillary pressure during a bubble penetrating from a tube into a mesh pore [13]; c: modulation of stratified flow in horizontal tube [13]; d: modulation of flow pattern in vertical tube with membrane tube insert [15]). Subfigures a–c are reprinted with permission from Ref. [13], Elsevier. Subfigure d is reprinted with permission from Ref. [15], Elsevier.

model" establishes the connection between "eye-blinking" oscillation and wall temperatures [17].

$$T_w = T_{w,ave} + T_{w,osc} = T_{w,ave} + \frac{q l_{unit} s_n (W + W_{porous})}{m_s C_{p,s}} \frac{\cos(2\pi f t) - 1}{2\pi f} \tag{20}$$

where the subscripts of w, ave and osc refer to wall, average and oscillation, respectively, f is the eye-blinking frequency. Because the oscillation term is inversely proportional to the oscillation frequency of bubble confinement ratio, yielding ultra-stable wall temperatures. The measured oscillation amplitude of T_w is less than 0.1 K, satisfying the demand for high precision temperature control of electronic devices (see Fig. 3d). In one word, the micro-evaporator using pin fins porous walls completely stabilizes boiling flow and heat transfer. Li et al. [53] proposed a flow boiling device based on phase separation concept. The key components are micro-pin-fin fences in multiple channels, which fundamentally change the thermal-hydraulic boundary layer structure. Significantly high heat transfer coefficient without elevating pressure drop was achieved.

Large pressure drop of two-phase flow is another problem for microchannel evaporator. Pressure drop is related to vapor mass quality or void fraction. The higher the vapor mass quality, the larger the pressure drop is. Vapor venting microchannel evaporator was investigated by Prof. Goodson KE's team from Stanford University [54]. In such a design, parallel microchannels are covered with a hydrophobic nano-membrane. Based on the principle of minimum surface energy, vapor tends to flow through the hydrophobic membrane and escape out of microchannels. Meanwhile, liquid is restricted in microchannels by large capillary pressure due to vapor-liquid interface in hydrophobic nanopores. The above design ensures the evaporator to operate at an extremely low vapor mass quality, thus the flow resistance is significantly reduced. Considering vapor permeability, leak protection of liquid and thermal stability of hydrophobic nano-membrane, the Teflon/nylon material with pore diameter of ~100 nm is recommended as the separating material [55], reaching a separation efficiency of 95% and a maximum drag reduction of 60% [55–57].

The phase separation for evaporator applications has following benefits: (1) The saturation temperature of fluid is reduced by vapor venting, which is useful to decrease wall temperatures. (2) The Ledinegg flow instability can be eliminated by vapor venting due to the changed hydraulic demand curve of pressure drops versus mass flow rates. (3) Higher flow rate of coolant can be supplied by the pump with the same pumping power. Hence, *CHF* can be increased.

Woodcock et al. [58] proposed a phase separation microchannel evaporator. The evaporator is fabricated by MEMS technique including 3D Piranha Pin Fins (PPF) array. Each pin fin contains an

open inlet mouth and a cavity volume which is connected with outside fluid. During the operation of evaporator, bubbles can be nucleated and growing in the tail region of a front pin fin. These bubbles, however, can be captured by the inlet mouth of a downstream pin fin and then discharged out of the pin fin cavity. The inlet mouth size, the bubble nucleation location and the 3D configuration of the pin fins were optimized [59–61]. The third generation of "Piranha" fin microchannel evaporator achieved *CHF* of ~1000 W/cm^2 with chip temperature lower than 95 °C [62], demonstrating advantages of using phase separation principle and "Piranha" fins array to increase *CHF*.

4.3. Phase separation for micro-condenser

Micro pin fins are integrated into micro heat exchanger to enhance heat transfer [63–65]. The uniformly populated pin fins array increases flow resistance while enhancing heat transfer. The phase separation micro-condenser was invented and investigated in Ref. [18]. Lined pin fins array is populated in micro-condenser, forming vapor passage and liquid passage alternatively in width direction. The outlet cross-section of evaporator is open to discharge condensed liquid (see Fig. 4).

At the inlet of micro-evaporator, vapor condenses in both vapor passage and liquid passage. Liquid film exists on side walls of pin fins due to their hydraulic feature. The theoretical analysis and experiments show that pin fins have strong capability to absorb liquid. When liquid in vapor passage contacts with side walls of pin fins, the vapor-liquid interface is advancing towards the throat location of pin fins, driven by free surface energy. Thus, liquid in vapor passage is captured by liquid in liquid passage. Meanwhile, vapor in liquid passage is condensed. In such a way, the phase separation is fulfilled with liquid in liquid passage and vapor in vapor passage. The lined pin fins act as the separation membrane.

A theoretical relationship is established between pressure drop and interfacial area between the two-phases. Phase separation greatly decreases interfacial area between the two-phases to reduce frictional pressure drops. The experiments in Ref. [18] shows that at the same pumping power, mass flow rate for phase separation condenser can be increased by 15%, compared to conventional condenser using solid wall microchannels. In other words, the phase separation condenser has the strong capability to decrease pressure drops.

It is noted that the mass flow rate of liquid increases along flow length. In order to consider the effect of added mass flow rate of liquid on phase separation, three micro-condensers were tested: solid wall microchannels micro-condenser (SWM), parallel phase separation condenser (PPS with constant cross sections of fluid passages) and conical phase separation condenser (CPS with varied cross sections of fluid passages), see Fig. 4a. With flow evolution for PPS, the cross sectional area of liquid passage is not sufficient to transport the mass flow rate of liquid. Hence, liquid is not only occupied in liquid passage, but also occupied in a portion of vapor passage, yielding pin fins immersed by liquid to make pin fins not effective for filmwise condensation (see Fig. 4b). However, the overflooding effect does not occur with CPS (see Fig. 4c). Because the increased flow rate of liquid is compensated by the enlarged cross sectional area of liquid passage, the vapor-liquid interface is pinned along the lined pin fins. The two side walls of pin fins facing vapor passage is exposed in vapor to perform effective filmwise condensation. Compared with SWM, CPS increases heat flux and heat transfer coefficient by 50% and 75%, respectively (see Fig. 4d–e).

4.4. Phase separation for large size condenser

Thick liquid film deteriorates condensation heat transfer. How to maintain thin liquid film condensation is an important topic. For example, the condensation heat transfer coefficient of organic fluid is even smaller than the convective heat transfer coefficient of single-phase water [66]. Phase separation condenser with gravity effect was proposed [40], in which flowing vapor condenses in downward tube bundles, until the condensed liquid reaches condenser bottom and then is extracted out of condenser. The residual vapor turns to flow upwards and condenses into liquid. Phase separation condenser using gravity effect is simple and reliable, increasing condensation heat transfer coefficients by 50% maximally, compared with overall downward condenser. Oh et al. [41] proposed an invention for multistage gas and liquid phase separation condenser, with tube bundles horizontally positioned. Fresh vapor enters the middle part of tube bundles and condenses there. Phase separation is functioned with the gravity effect. The condensed liquid enters a collection chamber and is further cooled in the bottom part of tube bundles [67]. Meanwhile, the separated vapor enters the top part of tube bundles and condenses there. An alternative design is to arrange vapor entering the top of a condenser. Vapor condenses in downward tube bundles. The condensed liquid is extracted from the bottom of the condenser [42]. The separation efficiency, heat transfer coefficient and pressure drop have been investigated for gravity driven phase separation condensers, showing better performance than conventional condensers [68–71].

Gravity driven phase separation has some limitations. First, the separation is only effective after liquid is accumulated to a specific amount in a channel. In other words, gravity driven is not an in-situ process. Second, in order to make the separation process effective, the pressure in a condenser tube should be large than the environment pressure where the condensed liquid is moved to. Alternatively, Ref. [12] presented a capillary driven phase separation. A set of adiabatic air-water experiments [13–15], condensing experiments with organic fluid as working fluid [16,72–74], multiscale numerical simulations [75–77], and prototype demonstration [78] were conducted. In mechanical engineering, metallic (copper, stainless steel) mesh screen, fabricated by textile technique, behaves lost cost for large scale utilizations. Compared with conventional method of sintering mesh screen on tube wall, the key idea is to suspend mesh screen membrane tube in a condenser tube, dividing tube cross-section into an annular region near the wall, and a core region inside the membrane tube. Vapor is confined in the annular region to form thin liquid film to enhance condensation heat transfer (see Fig. 5a). When a bubble interface is advancing from a larger space to a small space, the capillary pressure is (see Fig. 5b)

$$\Delta P_{12} = 4\gamma_{lv}\cos\theta\left(\frac{1}{d_p}-\frac{1}{D}\right) \tag{21}$$

where γ_{lv} is the surface tension and θ is the contact angle, d_p and D are the diameters of mesh pore and tube, respectively. Usually, a bubble is difficult to break through a mesh pore from a large tube due to large capillary pressure ($d_p \ll D$). For example, ΔP_{12} attains ~10 kPa with $d_p = 15$ μm, $D = 15$ mm and $\theta = 60^o$. This explains why bubbles prefer to be confined in annular region. On the other hand, liquid can be sucked into membrane tube. Thus, the in-situ separation from a vapor-liquid mixture is performed.

To verify the effectiveness of phase separation, air-water two-phase flow experiment was performed in a horizontal tube [13,14]. In horizontal tube without insert, stratified flow dominates at low flow rates of the two-phases, under which liquid is populated in the

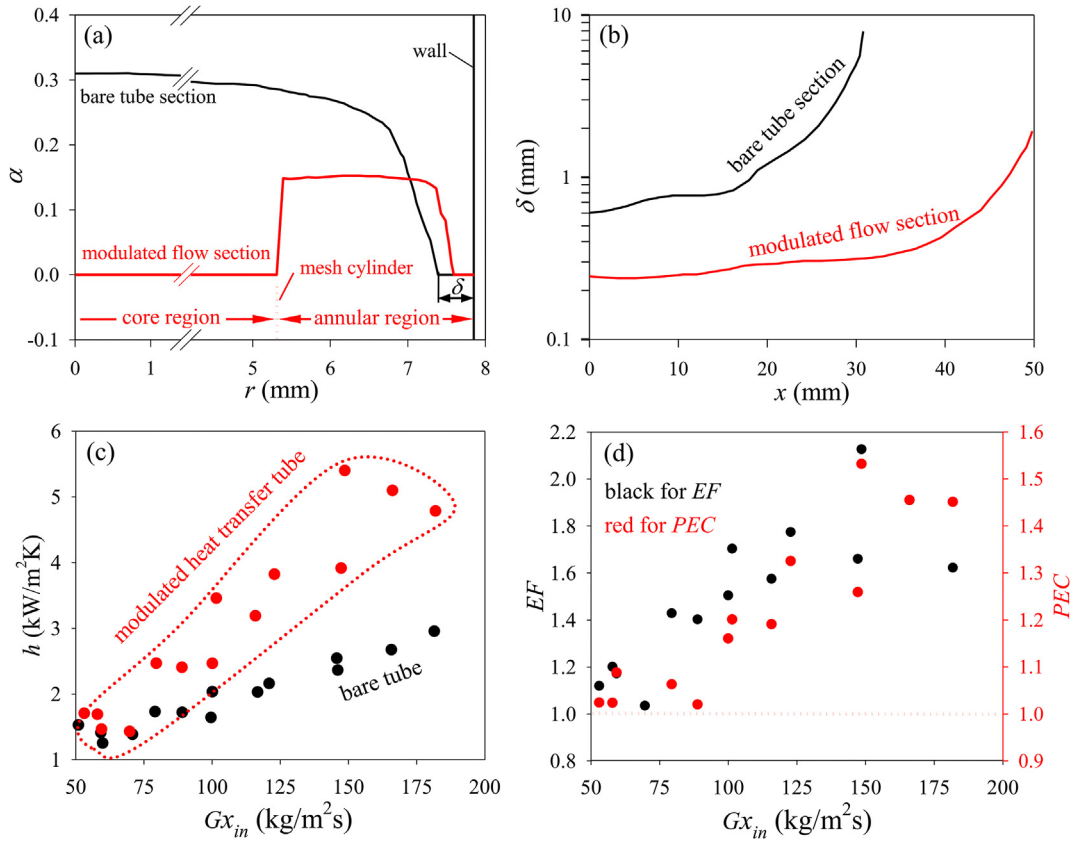

Fig. 6. Outcomes for phase separation condenser (a: void fraction α over the tube cross section [75]; b: liquid film thicknesses δ [75]; c: heat transfer coefficients h [72]; (d): heat transfer enhancement ratio *EF* and performance evaluation coefficient *PEC* [72]). Subfigures a and b are reprinted with permission from Ref. [75], Elsevier. Subfigures c and d are reprinted with permission from Ref. [72], Elsevier.

bottom part of the tube and gas is above the liquid interface. For practical applications, because a large proportion of tube cross-section is covered by liquid, stratified flow is not effective for condensation heat transfer. For phase separation tube, it is observed that liquid can be captured by mesh screen membrane, leaving more cross-section area of the tube exposed by gas, forming the "liquid levitation by gas" phenomenon (see Fig. 5c). For flow pattern modulation at higher flow rates, saddle bubbles are observed in annular region to create thin liquid film on tube wall. Subsequently, the two-phase experiment in vertical tube was performed [15]. Any bubbles are prevented from entering membrane tube but stay in annular region (see Fig. 5d). Due to large density difference between liquid and gas, a pulsating flow is self-sustained in membrane tube, increasing mass and momentum exchanges between annular region and core region, which is the second mechanism to enhance heat transfer except the thin film enhanced heat transfer. Numerical simulations show that the core region is occupied by liquid, and the (gas) void fraction in annular region significantly increases (see Fig. 6a). Liquid film thickness becomes thinner after flow pattern modulation (see Fig. 6b) [75].

Comparative convection condensation experiments were performed using a bare tube without insert and a phase separation condenser tube with a membrane tube insert [72]. Water and R245fa were the working fluids. Both test tubes were 1200 mm for effective condensation length and 14.81 mm for inner diameter of condenser tube. Two layers of mesh screen were used to fabricate the membrane tube insert, with a pore diameter of 76 μm for outer layer of the membrane tube. For stratified flow modulation, the membrane tube captures liquid to ensure more wall surface area of condenser tube covered by vapor to increase condensing heat transfer coefficients. For annular flow modulation, the membrane tube not only confines vapor in annular region near the tube wall, but also captures liquid droplets entrained in vapor to raise void fractions near tube wall. Phase separation condenser tube increases heat transfer coefficients to be two times of those of bare tube without membrane tube insert. The performance evaluation coefficient *PEC* is larger than 1, indicating that the phase separation condenser tube can be used for practical engineering (see Fig. 6c–d).

Further investigation involves the demonstration of a phase separation condenser, which was integrated in an Organic Rankine cycle to dissipate extra heat of the system to environment. During the operation of the machine, the phase separation condenser decreases the total thermal resistance of condensation by 45.6%, compared with a conventional condenser without membrane tube insert. Effect of different gravity levels on the effectiveness of phase separation condensation was explored. Especially, under micro-gravity environment, thick liquid film severely deteriorates condensation heat transfer [76,77]. Multiscale computations show that under micro-gravity environment, the liquid film thickness in phase separation tube can be 1/10–1/30 of that in bare tube without membrane tube insert.

4.5. Phase separation for smart heat pipe

Heat pipe has a strong coupling between evaporation and condensation. Phase distribution makes evaporator or condenser to choose their pathways working according to nucleate mechanism

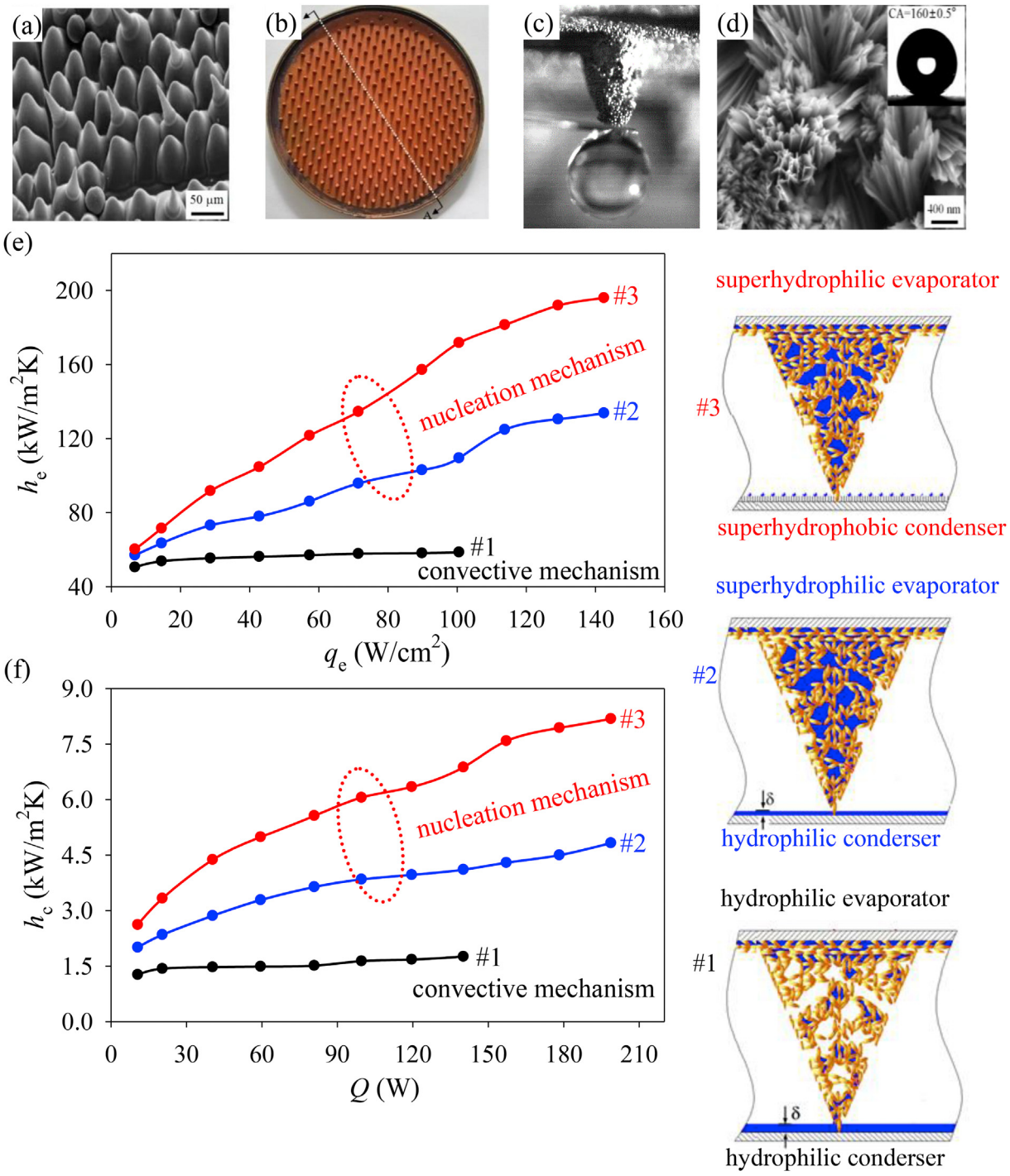

Fig. 7. Heat pipe based on phase separation principle [19] (a: mastoid processes of ruellia devosiana surface; b: evaporator with mastoid processes array sintered on copper substrate; c: anti-gravity suction of liquid by mastoid process; d: nanostructures on superhydrophobic condenser surface; (e): heat transfer coefficients of evaporator for the three heat pipe samples; f: heat transfer coefficients of condenser for the three heat pipe samples). Reprinted with permission from Ref. [19], Elsevier.

or convection mechanism, thus influencing the heat pipe performance. Evaporator behaves nucleate boiling mechanism at small vapor mass qualities, but convection mechanism at large vapor mass qualities. On the contrary, condenser behaves drop nucleation mechanism with vapor covering on the surface, but convection mechanism with liquid spreading on the surface. Usually, heat transfer coefficients increase with increase of heat fluxes with nucleate mechanism, but are not sensitive to the variation of heat loads with convection mechanism.

The connection between heat transfer mechanism and phase distribution inspires us to modulate phase distribution [19]. Once the phase distribution is adjusted to make evaporator working in nucleate boiling mechanism, and condenser working in drop nucleation mechanism, heat transfer coefficients increase with increases of heat loads for both components. This idea creates a new invention of smart heat pipe, having self-adaptive function to

follow the variation of external heat loads, which is attractive for industry applications [19].

Comparative experiments were performed by fabricating three samples of flat plate heat pipe. Inspired by mastoid processes array of ruellia devosiana surface in nature, the evaporator was made by sintering copper powders on copper substrate to form 3D array structure (see Fig. 7a–b). After sintering, mastoid processes are hydrophilic to capture water under anti-gravity operation. Nanostructure modification enhances the water absorption capability (see Fig. 7c). Condenser is a flat copper surface with and without nanostructure modification, see Fig. 7d for nanostructure. The heat pipe ensures direct contact of the tips of mastoid process of evaporator with the condenser surface.

The #1 sample has equal wettability of evaporator and condenser without nanostructure modification. The #2 sample has superhydrophilic evaporator with nanostructure modification and hydrophilic condenser without nanostructure modification. The #3 sample includes superhydrophilic evaporator and superhydrophobic condenser, behaving inverse wettability with nanostructures modification for both components. Phase distributions are discussed assuming same charged liquid in heat pipes. For the #1 sample, part of porous media is occupied by liquid, with the remain liquid spreading on condenser surface. The #2 sample has similar phase distribution, but the liquid film thickness on condenser surface decreases compared with the #1 sample. The #3 sample has different phase distribution, with the evaporator porous flooded by liquid and the condenser surface exposed by vapor. Hence, the #3 sample holds nucleate mechanism for evaporator and condenser, supported by measurements. Heat transfer coefficients are increased with increase of heat fluxes q_e for evaporator and heat loads Q for condenser (see Fig. 7e–f). However, the #1 sample does not change heat transfer coefficients with variations of heat loads. At a heat flux of ~100 W/cm^2 and on a 1.4 cm^2 heating area, the #3 sample decreases the hot spot temperature by 30–40 K, compared with the #1 sample.

5. Perspective of phase separation for energy utilizations

The energy and power industry creates various extreme conditions to dissipate ultra-high heat fluxes. For example, the heat flux supplied by fusion reactor approaches 10 kW/cm^2 [79]. Another example is the high concentration solar receiver whose heat flux is also very high. Phase change heat transfer is the most effective one, under which how to prevent the heater surface from dry-out is a challenge. Phase separation is useful for such functions. Specific attentions will be paid on the phase separation applied to extreme conditions.

Future works are suggested on the optimization of phase separation phase change heat transfer. Phase separation involves various geometry parameters and wettability parameters such as contact angle between solid material and working liquid. The optimization of phase separation obtains the largest degree of heat transfer enhancement. Usually, heat transfer enhancement accompanies a rise of pressure drops. Phase separation heat transfer system should be optimized to decrease the penalty of the rise of pressure drop. There are several issues such as flow instability, occurrence of critical heat flux and large pressure drop. Usually, a phase separation technique is difficult to overcome all the issues. Future works will be recommended on the phase separation to have multi-functions.

Base materials for phase change device can be metal, silicon and polymer. Phase separation heat transfer device should be fulfilled with the help of micro/nano fabrication technique, which is developing very fast. Future works are recommended on using various micro/nano fabrication techniques to make the phase separation heat transfer system.

6. Conclusions

Phase change heat transfer including boiling and condensation is important for efficient energy utilizations. The complicated mass, momentum and energy exchanges between the two-phases generate serious issues such as large pressure drop, occurrence of critical heat flux, and flow instability, which should be avoided for practical operation. Adapting to various applications, phase change heat transfer should increase heat transfer coefficients, suppress flow instabilities and delay the occurrence of critical heat flux. Phase separation is effective to improve the performance of phase change heat transfer. The present paper presents a comprehensive review on phase separation for phase change heat transfer. Conclusions are summarized as follows:

- When a bubble interface is crossing the junction interface between a large pore and a small pore, the bubble is advancing into small pores to generate phase separation due to the decrease of surface energy, which is attractive for applications due to the passive process.
- Using multiscale powders sintering or evaporation momentum force could generate phase separation. Phase separation assigns reasonable pathways for liquid and vapor, avoiding the countercurrent flow for the mixture transportation. Hence, heat transfer coefficients and critical heat fluxes are raised.
- Two-phase flow instability is more serious for microchannel boiling compared with that in large size channels. Using porous-wall microchannels to replace solid wall microchannels separates the two-phases, and promotes pressure transfer between different channels to eliminate bubble blockage. Thus, two-phase flow instability can be suppressed.
- Lined pin fins array generates phase separation for micro-condenser. Conical phase separation passage successfully adapts increased flow rate of liquid to raised cross sectional area of liquid passage along flow length. Vapor-liquid interface is pinned along pin fins array to make pin fins effective for film-wise condensation, presenting better performance for micro-condenser.
- The wettability match of superhydrophilic evaporator and superhydrophobic condenser modulates liquid to be populated in porous media of evaporator and vapor to be covered on condenser surface, creating nucleate boiling mechanism for evaporator and drop nucleation mechanism for condenser. Heat transfer coefficients are increased with increase of external heat loads for both components to invent smart heat pipe.
- Perspective research and development on phase separation are proposed including materials and applications.

Credit author statement

Xiaojing Ma: Validation, Investigation, Writing – original draft, Visualization; Jinliang Xu: Conceptualization, Resources, Writing – review & editing, Supervision; Jian Xie: Methodology, Writing – review & editing, Project administration, Funding acquisition.

Declaration of competing interest

The authors declare that they have no known competing financial interests or personal relationships that could have appeared to influence the work reported in this paper.

Acknowledgement

The study was supported by the National Natural Science Foundation of China (51821004 and 51806065) and Fundamental Research Funds for Central Universities (2020DF002).

References

[1] Collier JG, Thome JR. Convective boiling and condensation. third ed. New York: Oxford University Press; 1994.
[2] Chen JC. Correlation for boiling heat transfer to saturated fluids in convective flow. Ind Eng Chem Process Des Dev 1966;5:322–9.
[3] Kandlikar SG. High flux heat removal with microchannels—a roadmap of challenges and opportunities. Heat Tran Eng 2005;26:5–14.
[4] Ho CK, Iverson BD. Review of high-temperature central receiver designs for concentrating solar power. Renew Sustain Energy Rev 2014;29:835–46.
[5] Cavallini A, Del Col D, Doretti L, Longo GA, Rossetto L. Heat transfer and pressure drop during condensation of refrigerants inside horizontal enhanced tubes. Int J Refrig 2000;23:4–25.
[6] Srimuang W, Amatachaya P. A review of the applications of heat pipe heat exchangers for heat recovery. Renew Sustain Energy Rev 2012;16:4303–15.
[7] Huang G, Zhu Y, Liao ZY, Huang Z, Jiang PX. Transpiration cooling with bio-inspired structured surfaces. Bioinspiration Biomimetics 2020;15:036016.
[8] Chen Y, Sobhan CB, Peterson GP. Review of condensation heat transfer in microgravity environments. J Thermophys Heat Tran 2006;20:353–60.
[9] Laohalertdecha S, Wongwises S. Condensation heat transfer and flow characteristics of R-134a flowing through corrugated tubes. Int J Heat Mass Tran 2011;54:2673–82.
[10] Xie J, Xu J, Li X, Liu H. Dropwise condensation on superhydrophobic nanostructure surface, Part I: long-term operation and nanostructure failure. Int J Heat Mass Tran 2019;129:86–95.
[11] Chen X, Ye H, Fan X, Ren T, Zhang G. A review of small heat pipes for electronics. Appl Therm Eng 2016;96:1–17.
[12] Chen H, Xu J, Wang W. Internal liquid separating hood-type condensation heat exchange tube. United States Patent US9097470B2; 2015. Aug 4.
[13] Chen H, Xu J, Li Z, Xing F, Xie J. Stratified two-phase flow pattern modulation in a horizontal tube by the mesh pore cylinder surface. Appl Energy 2013;112:1283–90.
[14] Chen H, Xu J, Li Z, Xing F, Xie J, Wang W, et al. Flow pattern modulation in a horizontal tube by the passive phase separation concept. Int J Multiphas Flow 2012;45:12–23.
[15] Chen H, Xu J, Xie J, Xing F, Li Z. Modulated flow patterns for vertical upflow by the phase separation concept. Exp Therm Fluid Sci 2014;52:297–307.
[16] Xie J, Xu J, Liang C, She Q, Li M. A comprehensive understanding of enhanced condensation heat transfer using phase separation concept. Energy 2019;172:661–74.
[17] Xu J, Yu X, Jin W. Porous-wall microchannels generate high frequency “eye-blinking” interface oscillation, yielding ultra-stable wall temperatures. Int J Heat Mass Tran 2016;101:341–53.
[18] Yu X, Xu J, Yuan J, Zhang W. Microscale phase separation condensers with varied cross sections of each fluid phase: heat transfer enhancement and pressure drop reduction. Int J Heat Mass Tran 2018;118:439–54.
[19] Ji X, Xu J, Li H, Huang G. Switchable heat transfer mechanisms of nucleation and convection by wettability match of evaporator and condenser for heat pipes: nano-structured surface effect. Nanomater Energy 2017;38:313–25.
[20] Zuber N. Hydrodynamic aspects of boiling heat transfer. Doctoral Dissertation of University of California; 1959.
[21] Polezhaev YV, Kovalev S. Modelling heat transfer with boiling on porous structures. Therm Eng 1990;37:617–20.
[22] Liter SG, Kaviany M. Pool-boiling CHF enhancement by modulated porous-layer coating: theory and experiment. Int J Heat Mass Tran 2001;44:4287–311.
[23] Yin L, Jiang P, Xu R, Hu H, Jia L. Heat transfer and pressure drop characteristics of water flow boiling in open microchannels. Int J Heat Mass Tran 2019;137:204–15.
[24] Ruspini LC, Marcel CP, Clausse A. Two-phase flow instabilities: a review. Int J Heat Mass Tran 2014;71:521–48.
[25] Wu HY, Cheng P. Boiling instability in parallel silicon microchannels at different heat flux. Int J Heat Mass Tran 2004;47:3631–41.
[26] Xu J, Zhou J, Gan Y. Static and dynamic flow instability of a parallel microchannel heat sink at high heat fluxes. Energy Convers Manag 2005;46:313–34.
[27] Lyu Z, Xu J, Yu X, Jin W, Zhang W. Wavelet decomposition method decoupled boiling/evaporation oscillation mechanisms over two to three timescales: a study for a microchannel with pin fin structure. Int J Multiphas Flow 2015;72:53–72.
[28] Wang G, Cheng P, Bergles AE. Effects of inlet/outlet configurations on flow boiling instability in parallel microchannels. Int J Heat Mass Tran 2008;51:2267–81.
[29] Parmar R, Majumder SK. Hydrodynamics of microbubble suspension flow in pipes. Ind Eng Chem Res 2014;53:3689–701.
[30] Graham DM, Chato JC, Newell TA. Heat transfer and pressure drop during condensation of refrigerant 134a in an axially grooved tube. Int J Heat Mass Tran 1999;42:1935–44.
[31] Son CH, Oh HK. Condensation heat transfer characteristics of CO_2 in a horizontal smooth-and microfin-tube at high saturation temperatures. Appl Therm Eng 2012;36:51–62.
[32] Zhang L, Yang S, Xu H. Experimental study on condensation heat transfer characteristics of steam on horizontal twisted elliptical tubes. Appl Energy 2012;97:881–7.
[33] Moghaddam HA, Sarmadian A, Asnaashari A, Han Joushani, Islam MS, Saha SC, et al. Condensation heat transfer and pressure drop characteristics of Isobutane in horizontal channels with twisted tape inserts. Int J Refrig 2020;118:31–40.
[34] Khatua AK, Kumar P, Singh HN, Kumar R. Measurement of enhanced heat transfer coefficient with perforated twisted tape inserts during condensation of R-245fa. Heat Mass Tran 2016;52:683–91.
[35] Nusselt W. Die oberflachenkondensation des wasserdamphes. VDI-Zs 1916;60:541.
[36] Ramesh KN, Sharma TK, Rao GAP. Latest Advancements in heat transfer enhancement in the micro-channel heat sinks: a review. Arch Comput Methods Eng 2020. https://doi.org/10.1007/s11831-020-09495-1.
[37] Tang J, Hu X, Yu Y. Electric field effect on the heat transfer enhancement in a vertical rectangular microgrooves heat sink. Int J Therm Sci 2020;150:106222.
[38] Goshayeshi HR, Goodarzi M, Safaei MR, Dahari M. Experimental study on the effect of inclination angle on heat transfer enhancement of a ferrofluid in a closed loop oscillating heat pipe under magnetic field. Exp Therm Fluid Sci 2016;74:265–70.
[39] Yu F, Luo X, He B, Xiao J, Wang W, Zhang J. Experimental investigation of flow boiling heat transfer enhancement under ultrasound fields in a minichannel heat sink. Ultrason Sonochem 2021;70:105342.
[40] Peng XF, Jia L. Steam-water heat exchanger with constant flow velocity. Chinese Patent CN 1401966 A 2003. Mar 12.
[41] Oh K, Lee S, Park T, Kim Y. Multistage gas and liquid phase separation condenser. United States Patent US6769269B2; 2004. Aug 3.
[42] Zeng X, Ye L. Condenser. Chinese Patent CN101021376 A 2007. Aug 22.
[43] Kandlikar SG. Controlling bubble motion over heated surface through evaporation momentum force to enhance pool boiling heat transfer. Appl Phys Lett 2013;102:051611.
[44] Jaikumar A, Kandlikar SG. Ultra-high pool boiling performance and effect of channel width with selectively coated open microchannels. Int J Heat Mass Tran 2016;95:795–805.
[45] Yu X, Xu J, Liu G, Ji X. Phase separation evaporator using pin-fin-porous wall microchannels: comprehensive upgrading of thermal-hydraulic operating performance. Int J Heat Mass Tran 2021;164:120460.
[46] Ji X, Xu J, Zhao Z, Yang W. Pool boiling heat transfer on uniform and non-uniform porous coating surfaces. Exp Therm Fluid Sci 2013;48:198–212.
[47] Dai X, Yang F, Yang R, Lee YC, Li C. Micromembrane-enhanced capillary evaporation. Int J Heat Mass Tran 2013;64:1101–8.
[48] Rahman MM, Pollack J, McCarthy M. Increasing boiling heat transfer using low conductivity materials. Sci Rep 2015;5:13145.
[49] Ma X, Cheng P, Quan X. Simulations of saturated boiling heat transfer on bio-inspired two-phase heat sinks by a phase-change lattice Boltzmann method. Int J Heat Mass Tran 2018;127:1013–24.
[50] Xu J, Ji X, Yang W, Zhao Z. Modulated porous wick evaporator for loop heat pipes: Experiment. Int J Heat Mass Tran 2014;72:163–76.
[51] Ji X, Wang Y, Xu J, Huang Y. Experimental study of heat transfer and start-up of loop heat pipe with multiscale porous wicks. Appl Therm Eng 2017;117:782–98.
[52] Zhao YP. Physical mechanics of surface and interface. Beijing: Science Press; 2012 [in Chinese)].
[53] Li W, Wang Z, Yang F, Alam T, Jiang M, Qu X, et al. Supercapillary architecture-activated two-phase boundary layer structures for highly stable and efficient flow boiling heat transfer. Adv Mater 2019;32:1905117.
[54] Zhou P, Goodson K, Suntiago J. Vapor escape microchannel heat exchanger. United States Patent US6994151B2; 2006 Feb 7.
[55] David MP, Miler J, Steinbrenner JE, Yang Y, Touzelbaev M, Goodson KE. Hydraulic and thermal characteristics of a vapor venting two-phase microchannel heat exchanger. Int J Heat Mass Tran 2011;54:5504–16.
[56] Marconnet AM, David MP, Rogacs A, Flynn RD, Goodson KE. Temperature-dependent permeability of microporous membranes for vapor venting heat exchangers. ASME International Mechanical Engineering Congress and Exposition 2008. Oct 31-Nov 6; Boston, USA. IMECE2008-67934.
[57] David MP, Khurana T, Hidrovo C, Pruitt BL, Goodson KE. Vapor-venting, micromachined heat exchanger for electronics cooling. ASME International Mechanical Engineering Congress and Exposition 2007. Nov 11-15; Washington, USA. IMECE2007-42553.
[58] Woodcock C, Houshmand F, Plawsky J, Izenson M, Fogg D, Hill R, et al. Piranha Pin-Fins (PPF): voracious boiling heat transfer by vapor venting from microchannels-system calibration and single-phase fluid dynamics. May 27-30; Orlando USA. In: Fourteenth intersociety conference on thermal and thermomechanical phenomena in electronic systems; 2014. p. 282–9.
[59] Woodcock C, Yu X, Plawsky J, Peles Y. Piranha Pin Fin (PPF)—advanced flow boiling microstructures with low surface tension dielectric fluids. Int J Heat Mass Tran 2015;90:591–604.
[60] Yu X, Woodcock C, Plawsky J, Peles Y. An investigation of convective heat transfer in microchannel with Piranha Pin Fin. Int J Heat Mass Tran 2016;103:

1125–32.
[61] Yu X, Woodcock C, Wang Y, Plawsky J, Peles Y. Enhanced subcooled flow boiling heat transfer in microchannel with Piranha Pin Fin. J Heat Tran 2017;139:112402.
[62] Woodcock C, Ng'oma C, Sweet M, Wang Y, Peles Y, Plawsky J. Ultra-high heat flux dissipation with Piranha pin fins. Int J Heat Mass Tran 2019;128:504–15.
[63] Xu F, Wu H. Experimental study of water flow and heat transfer in silicon micro-pin-fin heat sinks. J Heat Tran 2018;140:122401.
[64] Jia Y, Xia G, Li Y, Ma D, Cai B. Heat transfer and fluid flow characteristics of combined microchannel with cone-shaped micro pin fins. Int Commun Heat Mass Tran 2018;92:78–89.
[65] Cao Z, Liu B, Preger C, Wu Z, Zhang Y, Wang X, et al. Pool boiling heat transfer of FC-72 on pin-fin silicon surfaces with nanoparticle deposition. Int J Heat Mass Tran 2018;126:1019–33.
[66] Dewan A, Mahanta P, Raju KS, Kumar PS. Review of passive heat transfer augmentation techniques. Proc IME J Power Energy 2004;218:509–27.
[67] Lee JK. Two-phase flow behavior inside a header connected to multiple parallel channels. Exp Therm Fluid Sci 2009;33:195–202.
[68] Wu D, Wang Z, Lu G, Peng X. High-performance air cooling condenser with liquid–vapor separation. Heat Tran Eng 2010;31:973–80.
[69] Chen Y, Hua N, Deng L. Performances of a split-type air conditioner employing a condenser with liquid–vapor separation baffles. Int J Refrig 2012;35:278–89.
[70] Zheng W, Chen Y, Hua N, Zhong T, Gong Y. Comparative performance of an automotive air conditioning system using micro-channel condensers with and without liquid-vapor separation. Energy Procedia 2014;61:1646–9.
[71] Chen Y, Deng L, Mo S, Luo X. Energy and exergy analysis on a parallel-flow condenser with liquid–vapor separators in an R22 residential air-conditioning system. Heat Tran Eng 2015;36:102–12.
[72] Xie J, Xu J, Xing F, Wang Z, Liu H. The phase separation concept condensation heat transfer in horizontal tubes for low-grade energy utilization. Energy 2014;69:787–800.
[73] Xie J, Xu J, Cheng Y, Xing F, He X. Condensation heat transfer of R245fa in tubes with and without lyophilic porous-membrane-tube insert. Int J Heat Mass Tran 2015;88:261–75.
[74] Xie J, Xing F, Xu J, Liu H. Significant heat transfer enhancement for R123 condensation by micromembrane cylinder. Chin Sci Bull 2014;59:3676–85.
[75] Chen Q, Xu J, Sun D, Cao Z, Xie J, Xing F. Numerical simulation of the modulated flow pattern for vertical upflows by the phase separation concept. Int J Multiphas Flow 2013;56:105–18.
[76] Sun D, Xu J, Chen Q, Yan Y. Modulated flow pattern in a condenser tube with two-phase flow interacting with mesh screen surface at micro-gravity. Int J Multiphas Flow 2015;69:54–62.
[77] Sun D, Xu J, Wang Y, Xie J, Xing F. Effect of gravity levels on the flow pattern modulation by the phase separation concept. Comput Fluids 2015;108:43–56.
[78] Cao S, Ji X, Xu J. R245fa condensation heat transfer in a phase separation condenser. Exp Therm Fluid Sci 2018;98:346–61.
[79] Raffray AR, Nygren R, Whyte DG, Abdel-Khalik S, Doerner R, Escourbiac F, et al. High heat flux components—readiness to proceed from near term fusion systems to power plants. Fusion Eng Des 2010;85:93–108.